

## Free-Energy Surfaces for Liquid-Phase Reactions and Their Use To Study the Border Between Concerted and Nonconcerted $\alpha,\beta$ -Elimination Reactions of Esters and Thioesters

Yongho Kim,<sup>†,‡</sup> Jerry R. Mohrig,<sup>§</sup> and Donald G. Truhlar<sup>\*,†</sup>

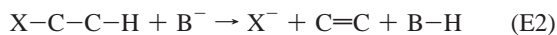
*Department of Chemistry and Supercomputing Institute, University of Minnesota, Minneapolis, Minnesota 55455-0431, Department of Chemistry, Kyung Hee University, Yongin-City, Gyeonggi-Do 449-701, Korea, and Department of Chemistry, Carleton College, Northfield, Minnesota 55057*

Received February 10, 2010; E-mail: truhlar@umn.edu

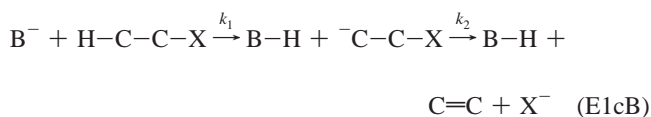
**Abstract:** Distinguishing between the concerted second-order mechanism for  $\beta$ -eliminations and nonconcerted mechanisms with discrete carbanion intermediates is very difficult experimentally, but the ability of quantum chemistry to find stationary points of the free-energy surface in liquid-phase solutions, even for complex reagents, provides a new tool for elucidating such mechanisms. Here we use liquid-phase density functional theory calculations to find transition states and intermediates on the free-energy surfaces of four base-initiated  $\alpha,\beta$ -eliminations of acetoxy and mesyloxy esters and their analogous thioesters. The geometries, free energies, and charge distributions of these structures support a stepwise irreversible first-order elimination from a conjugate base (E1cB<sub>I</sub>) mechanism with acetoxy ester **3**, acetoxy thioester **4**, and mesyloxy thioester **6**. However, mesyloxy ester **5**, which has an excellent nucleofuge and a less-acidic proton, follows a concerted but asynchronous E2 mechanism with an E1cB-like transition state. The anti transition state is more favorable than the syn one, even for the poorer nucleofuge and more-acidic thioesters. The article includes a general scheme for describing liquid-phase reactions in terms of free-energy surfaces.

### Introduction

Bordwell identified six classes of base-initiated alkene-forming elimination reactions,<sup>1</sup> and March distinguishes five.<sup>2</sup> We are particularly concerned here with concerted second-order elimination (E2),



and first-order elimination from a conjugate base (E1cB),



It should be noted that in the E1cB mechanism, the conjugate base of the substrate expels the nucleofuge; since the conjugate base is a carbanion, this mechanism is sometimes called the carbanion mechanism. When  $k_1$  is small and  $k_2$  is large, step 1 is essentially irreversible; this mechanism is called E1cB<sub>I</sub>, where the I subscript denotes “irreversible”. When the mechanism is E2, the reaction is concerted but dissociation of the proton and

the nucleofuge need not be synchronous; thus, the transition state may be carbanion-like (E1cB-like).

A classic problem in diagnosing mechanisms of these reactions has been distinguishing between the E2 pathway in which the transition state is E1cB-like on the one hand and the E1cB<sub>I</sub> pathway on the other.<sup>1–4</sup> Many attempts have been made to use kinetic isotope effects (KIEs) involving both the  $\alpha$  and  $\beta$  positions to solve this problem. However, the conclusions are often ambiguous because E2 mechanisms at the E1cB border can show many of the same characteristics as E1cB<sub>I</sub> mechanisms.

A comprehensive study by Ryberg and Matsson on the mechanism of base-promoted HF elimination from 4-fluoro-4-(4'-nitrophenyl)butan-2-one in aqueous methanol, which utilized primary and secondary deuterium KIEs as well as fluorine KIEs, was consistent with either an E1cB-like E2 mechanism or an E1cB<sub>I</sub> mechanism.<sup>5</sup> Further experimental study of the same substrate using double isotopic fractionation experiments demonstrated that the elimination proceeds via an E1cB<sub>I</sub> mechanism.<sup>6</sup> However, optimized stationary points, geometry changes along the solution-phase minimum free-energy path, and the solution-phase free-energy profile obtained from a recent computational study of this substrate suggested that the elimina-

<sup>†</sup> University of Minnesota.

<sup>‡</sup> Kyung Hee University.

<sup>§</sup> Carleton College.

(1) Bordwell, F. G. *Acc. Chem. Res.* **1972**, *5*, 374–381.

(2) Smith, M. B.; March, J. *March's Advanced Organic Chemistry*, 5th ed.; Wiley: New York, 2001; pp 1299–1322.

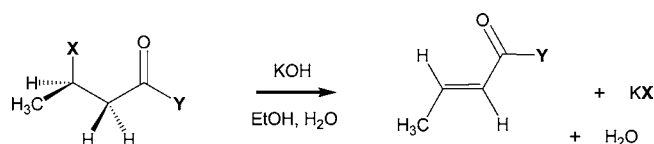
(3) Saunders, W. H., Jr. *Acc. Chem. Res.* **1976**, *9*, 19–25.

(4) Gandler, J. R. Mechanisms of Base-Catalyzed Alkene-Forming 1,2-Eliminations. In *The Chemistry of Doubly-Bonded Functional Groups*; Patai, S., Ed.; Wiley: New York, 1989; pp 733–797.

(5) Ryberg, P.; Matsson, O. *J. Am. Chem. Soc.* **2001**, *123*, 2712–2718.

(6) Ryberg, P.; Matsson, O. *J. Org. Chem.* **2002**, *67*, 811–814.

Scheme 1



	X	Y
<b>1a</b>	(CH <sub>3</sub> ) <sub>3</sub> CCO <sub>2</sub>	OC(CH <sub>3</sub> ) <sub>3</sub>
<b>1b</b>	(CH <sub>3</sub> ) <sub>3</sub> CCO <sub>2</sub>	SC(CH <sub>3</sub> ) <sub>3</sub>
<b>2a</b>		OC(CH <sub>3</sub> ) <sub>3</sub>
<b>2b</b>		SC(CH <sub>3</sub> ) <sub>3</sub>

tion reaction occurs concertedly but asynchronously via an E1cB-like transition state.<sup>7</sup>

The geometry of E2 transition states can be anti or syn,<sup>4,8</sup> and the fraction of reaction proceeding through each mode can be evaluated experimentally by studying the reactions of deuterium-labeled diastereomers.<sup>9</sup> Although the factors determining the preferred conformation of the transition state are not completely understood, the stereoelectronic argument<sup>10</sup> that orbital overlap in forming  $\pi$  bonds favors an anti arrangement for E2 transition states is widely accepted. However, both modes are observed experimentally.<sup>4,9,11</sup> It has been suggested that electron-withdrawing substituents (and thus more-acidic hydrogens) as well as poor nucleofuges produce transition states with more E1cB character, which are more favorable for syn elimination.<sup>4,12,13</sup> However, an increase in syn elimination for reactions close to the E1cB border was not observed<sup>14</sup> in a study of the KOH-catalyzed elimination of the stereospecifically deuterated 3-trimethylacetoxymethylbutanoate ester **1a** and its thioester analogue **1b** in 3:1 (v/v) ethanol/water solution (Scheme 1). Even at the E1cB border, there was only 5–6% intermolecular syn elimination,<sup>14</sup> the usual amount for acyclic substrates undergoing E2 reactions.

In a related study that also employed stereospecifically deuterated substrates, hydroxide-catalyzed 1,2-elimination reactions of *tert*-butyl 3-tosyloxybutanoate (**2a**) and its thioester analogue **2b** also produced only 5–6% syn elimination.<sup>15</sup> Because the tosyloxy group is an excellent nucleofuge, it was suggested that these reactions proceed via an E2 mechanism in which the transition state is E1cB-like rather than via an E1cB<sub>1</sub> mechanism.

A major reason for this computational study was to discover whether these substrates react by a concerted mechanism in

Table 1. Elimination Substrates Studied

substrate	X	Y
<b>3</b>	CH <sub>3</sub> CO <sub>2</sub>	OCH <sub>3</sub>
<b>4</b>	CH <sub>3</sub> CO <sub>2</sub>	SCH <sub>3</sub>
<b>5</b>	CH <sub>3</sub> SO <sub>2</sub> O	OCH <sub>3</sub>
<b>6</b>	CH <sub>3</sub> SO <sub>2</sub> O	SCH <sub>3</sub>

which the transition state is E1cB-like or by an E1cB<sub>1</sub> pathway in which a carbanion is a discrete intermediate at a significant energy minimum. In addition, we wished to see whether the stereochemical results from earlier experiments using stereospecifically deuterated (*2R*\*,*3R*\*)-**1a** and -**2a** and their (*2R*\*,*3S*\*) diastereomers as well as the analogous thioesters **1b** and **2b** could be modeled successfully by computational methods. In the experimental study of the stereospecifically deuterated reactants, it was surmised from KIE measurements and from the large amount of data that organic chemists have amassed on structure–reactivity relationships that the mechanism either was concerted with an E1cB-like transition state or was an E1cB<sub>1</sub> pathway. A reversible E1cB<sub>R</sub> pathway was excluded because there was no H–D exchange at the  $\alpha$ -position during the elimination reaction.<sup>14,15</sup>

The ultimate deciding feature in regard to whether the mechanism is E2 or E1cB is that the latter has a kinetically significant intermediate and the former does not. Furthermore, in the case of the E1cB<sub>1</sub> mechanism, the intermediate is present only in steady-state concentrations. In liquid-phase solution at thermodynamic equilibrium, the existence of an intermediate is determined by the topography of the concentration-dependent potential of mean force, which is also called the free-energy surface (FES). Here we employed electronic structure calculations in the liquid state to explore the FES for elimination reactions at the E1cB border by finding the stationary points of each FES. In particular, we calculated structures for reactants, products, intermediates, and transition states of 1,2-elimination reactions of the four  $\beta$ -substituted butanoic acid derivatives listed in Table 1: methyl 3-acetoxymethylbutanoate (**3**), methyl 3-acetoxymethylbutanethioate (**4**), methyl 3-mesyloxybutanoate (**5**), and methyl 3-mesyloxybutanethioate (**6**). Hydroxide anion was chosen as the base, and the solvent was a 1:1 (mol/mol) ethanol/water mixture, which is the mole ratio for a 3:1 (v/v) ethanol/water mixture. All four reactions lead to a product alkene in which the methyl group is *trans* (*E*) to the carbonyl, but the systematic functional group variation can lead to different behaviors in other respects. In particular, the thioesters **4** and **6** are stronger acids, and **5** and **6** have better nucleofuges; thus, the elimination reaction of **5** should be most E2-like and that of **4** most E1cB-like, with **3** and **6** displaying intermediate behavior.

For an *N*-atom solute or supersolute (where a supersolute is a solute plus one or more solvent molecules that are treated as part of the solute in order to better represent specific solute–solvent interactions or to maintain a given size of the “solute”), the FES is a function of  $3N - 6$  internal solute coordinates **R**, since it does not depend on the coordinates of the center of mass or the orientation. With a convenient choice for the zero of energy, the  $(3N - 6)$ -dimensional FES,  $W(\mathbf{R})$ , may be calculated as<sup>16–21</sup>

- (7) Kim, Y.; Marenich, A. V.; Zheng, J.; Kim, K. H.; Kolodziejska-Huben, M.; Rostkowski, M.; Paneth, P.; Truhlar, D. G. *J. Chem. Theory Comput.* **2009**, *5*, 324–333.
- (8) Gronert, S. *J. Am. Chem. Soc.* **1992**, *114*, 2349–2354.
- (9) Bartsch, R. A.; Zavada, J. *Chem. Rev.* **1980**, *80*, 453–494.
- (10) Bach, R. D.; Badger, R. C.; Lang, T. J. *J. Am. Chem. Soc.* **1979**, *101*, 2845–2848.
- (11) Sicher, J. *Angew. Chem., Int. Ed. Engl.* **1972**, *11*, 200–214.
- (12) Bickelhaupt, F. M.; Baerends, E. J.; Nibbering, N. M. M.; Ziegler, T. *J. Am. Chem. Soc.* **1993**, *115*, 9160–9173.
- (13) Saunders, W. H., Jr. *J. Org. Chem.* **2000**, *65*, 681–684.
- (14) Mohrig, J. R.; Carlson, J. R.; Coughlin, J. M.; Hofmeister, G. E.; McMartin, L. A.; Rowley, E. G.; Trimmer, E. E.; Wild, A. J.; Schultz, S. C. *J. Org. Chem.* **2007**, *72*, 793–798.
- (15) Mohrig, J. R.; Alberg, D. G.; Cartwright, C. H.; Pflum, M. K. H.; Aldrich, J. S.; Anderson, J. K.; Anderson, S. R.; Fimmen, R. L.; Snover, A. K. *Org. Biomol. Chem.* **2008**, *6*, 1641–1646.

- (16) Ben-Naim, A. *Statistical Thermodynamics for Chemists and Biochemists*; Plenum Press: New York, 1992; pp 314–321.
- (17) Truhlar, D. G.; Liu, Y.-P.; Schenter, G. K.; Garrett, B. C. *J. Phys. Chem.* **1994**, *98*, 8396–8405.
- (18) Garrett, B. C.; Schenter, G. K. *Int. Rev. Phys. Chem.* **1994**, *13*, 263–289.

$$W(\mathbf{R}) = V(\mathbf{R}) + \Delta G_S^*(\mathbf{R}) \quad (1)$$

where  $V(\mathbf{R})$  is the gas-phase potential energy surface and  $\Delta G_S^*(\mathbf{R})$  is the clamped-nuclei, fixed-concentration free energy of solvation [ $\Delta G_S^*$  is the standard-state free energy of solvation if we (unconventionally) take the standard-state concentration to be 1 mol/L in the gas phase as well as in the liquid). Equation 1 has very clear physical interpretation. In particular  $\Delta G_S^*(\mathbf{R})$  may be interpreted as the work of coupling a solute that is fixed in position to the equilibrated solvent at fixed temperature and pressure in an infinitely dilute solution.<sup>16</sup> (In contrast, the conventional standard-state solvation free energy,  $\Delta G_S^0$ , does not have this simple interpretation.) One could use the FES as the starting point for dynamics calculations,<sup>7,17–22</sup> but here we have based our analysis on finding and characterizing the stationary points of the FES and calculating their zero-point-exclusive and zero-point-inclusive relative free energies using a well-validated density functional<sup>23,24</sup> and continuum solvation model.<sup>25</sup>

### Theory

The liquid-phase FES defined in eq 1 is the same as the statistical mechanical potential of mean force.<sup>26,27</sup> It should be noted that the magnitude of  $W(\mathbf{R})$  would be shifted by a constant for a different choice of the zero of energy, which would correspond to using different standard concentrations for the free energy of solvation, but the geometry dependence of the potential of mean force does not depend directly on concentrations (although there is an indirect dependence since solvent properties depend on concentration for nondilute solutions). Therefore, for dilute solutions, the existence (or not) and character (stable or saddle) of the stationary points of the potential of mean force do not depend directly on concentrations. However, the free-energy differences between reagents (reactants or products), intermediates, and transition states do depend directly on concentrations if the numbers of moles differ. For dilute solutions, this dependence contains no information on solute–solvent coupling and cancels out in equilibrium constants for processes in which the number of moles does not change and in unimolecular rate constants; thus, our discussion of free-energy profiles should focus on physical quantities rather than artificial ones, and we will next explain how this can be done. The discussion is presented in general terms because we anticipate broad interest in this subject now that computational chemistry can make quantitatively useful predictions for reaction mechanisms in liquid-phase solutions.

We will use the term “arrangement” to denote a set of reactants or products or a unimolecular reactant, product, intermediate, or transition state when we make a statement or write an equation that refers generally to any of these cases.

Each arrangement is associated with a stationary point (structure) on the potential of mean force, and we will thus label a general arrangement as  $S$ , which denotes “structure.”

Consider a process in which an arrangement 1, consisting of  $n(1)$  species (which can be atoms, molecules, or clusters, charged or uncharged) is converted to another arrangement 2 (which could be a transition state, an intermediate, a product, or a set of products) consisting of  $n(2)$  species. For example,  $n(2) = 3$  for the final state of the E1cb mechanism displayed in the first paragraph of the Introduction. Let  $N_i(S)$  be the number of atoms in species  $i$  of arrangement  $S$ . We denote the reactant as  $S = \mathbf{R}$ , with  $n(\mathbf{R})$  equal to 2 for bimolecular reactions and 1 for unimolecular processes.

Let  $U(S)$  be the FES at a stationary point  $S$ , that is,

$$U(S) = W[\mathbf{R}(S)] \quad (2)$$

and let  $U_0(S)$  be the zero-point-inclusive FES at  $S$ , which we approximate as

$$U_0(S) \equiv U(S) + \frac{1}{2}\hbar \sum_{m=1}^{F(S)} \omega_m(S) \quad (3)$$

where

$$F(S) = \sum_{i=1}^{n(S)} [3N_i(S) - 6] \quad (4)$$

for stable structures [local minima of  $W(\mathbf{R})$ ] and

$$F(S) = 3N_i(S) - 7 \quad (5)$$

for transition structures [saddle points of  $W(\mathbf{R})$ ], which are assumed here to always have  $n(S) = 1$ , and where  $\omega_m(S)$  is the vibrational frequency of mode  $m$  of structure  $S$ . (It should be noted that  $\omega_m$  has units of radians/s; to use  $\text{cm}^{-1}$ ,  $\hbar$  would be replaced by  $hc$ .) By “zero-point-inclusive,” we mean that we have added the solute’s zero-point vibrational energy.

We next invoke Ben-Naim’s statistical thermodynamic interpretation of the solvation process. Ben-Naim writes  $G_i$ , the chemical potential (molar Gibbs free energy) of a species in a liquid-phase solution, as<sup>16</sup>

$$G_i = G_i^* - TS_{\text{lib},i} \quad (6)$$

where  $G_i^*$  is the chemical potential of a species whose center of mass is constrained to a fixed position in the solution,  $T$  is the absolute temperature, and  $S_{\text{lib},i}$  is the entropy of liberation species  $i$ , given by

$$S_{\text{lib},i} = -R \ln(C_i N_A \Lambda_i^3) \quad (7)$$

in which  $R$  is the gas constant,  $C_i$  is the concentration of  $i$  in moles per unit volume,  $N_A$  is Avogadro’s constant, and  $\Lambda_i$  is the concentration-independent thermal de Broglie wavelength, given by

$$\Lambda_i = h(2\pi m_i k_B T)^{-1/2} \quad (8)$$

where  $m_i$  is the mass of species  $i$  and  $k_B$  is Boltzmann’s constant. Ben-Naim labels  $G_i^*$  as the “pseudochemical potential,” and it may be associated with the internal free energy of the species in solution, including its coupling to the solvent.<sup>16</sup> The last term of eq 6, called the free energy of liberation,<sup>16</sup> is formally identical to the translational molar free energy in an ideal gas.

(19) Chuang, Y.-Y.; Cramer, C. J.; Truhlar, D. G. *Int. J. Quantum Chem.* **1998**, *70*, 887–896.

(20) Cramer, C. J.; Truhlar, D. G. *Chem. Rev.* **1999**, *99*, 2161–2200.

(21) Chuang, Y.-Y.; Truhlar, D. G. *J. Am. Chem. Soc.* **1999**, *121*, 10157–10167.

(22) Truhlar, D. G.; Pliego, J. R., Jr. In *Continuum Solvation Models in Chemical Physics: From Theory to Applications*; Mennucci, B., Cammi, R., Eds.; Wiley: Chichester, U.K., 2007; pp 338–365.

(23) Zhao, Y.; Truhlar, D. G. *Theor. Chem. Acc.* **2008**, *120*, 215–241.

(24) Zhao, Y.; Truhlar, D. G. *Acc. Chem. Res.* **2008**, *41*, 157–167.

(25) Marenich, A. V.; Olson, R. M.; Kelly, C. P.; Cramer, C. J.; Truhlar, D. G. *J. Chem. Theory Comput.* **2007**, *3*, 2011–2033.

(26) Kirkwood, J. G. *J. Chem. Phys.* **1935**, *3*, 300–313.

(27) McQuarrie, D. A. *Statistical Mechanics*; Harper & Row: New York, 1973; p 266.

One may approximate  $G^*$  in arrangement  $S$  as

$$G^*(S) = U_0(S) + G_{\text{int}}(S) \quad (9)$$

where  $G_{\text{int}}$  is the internal (i.e., electronic–vibrational–rotational and, if applicable, conformational) thermal free energy summed over  $i = 1$  to  $n(S)$ . By “thermal” we mean excluding the zero-point energy, which is already in  $U_0$ . It should be noted that in an instantaneous configuration of the solute, the rotations are converted to librations, which are low-frequency vibrations, but in the approximation of describing the solute dynamics by a potential of mean force, we average over the solvent, so  $W$  is independent of solute orientation and there are three free rotations. When  $S$  is a stable species (i.e., a local minimum of the FES), eqs 3, 4, and 9 define the usual free energy of that species in solution. When  $S$  is a saddle point of the FES, one omits the reaction coordinate not only in eq 5 (as we have already done) but also in  $G_{\text{int}}(S)$ , and eqs 3, 5, and 9 for saddle points extend conventional transition-state theory to the condensed phase. For higher accuracy, variational transition-state theory should be used,<sup>17–22,28,29</sup> but that is beyond the scope of the present article.

One can distinguish a hierarchy of theoretical levels. In the most approximate, called the separable-equilibrium solvation approximation,<sup>19–22</sup> one finds the stationary points of the solute gas-phase potential energy  $V$  and solvates them. However, in the approximation used here, which has been called the equilibrium solvation path method,<sup>18–22</sup> the stationary points of the pseudochemical potential surface (a free-energy surface with a particularly clear physical interpretation) are found. This is the most direct possible route to ascertaining the existence (or not) of intermediates and comparing the intrinsic favorableness of stereoisomeric transition states in liquid-state solutions. Even when one optimizes the structures based on the pseudochemical potential surfaces, as done here, one can consider three successively higher-level approximations to  $G^*$ , given by  $U$ ,  $U_0$ , and eq 9. Furthermore, in  $U_0$  and eq 9, one can use solution-phase frequencies computed from the Hessian of  $W$  or approximate them by gas-phase frequencies. In this article, we present results obtained using  $U_0$  with solution-phase frequencies; however, the Supporting Information also presents lower-level results based on  $U$ .

For any quantity  $Z$  (which may be  $G$ ,  $G^*$ , or  $S_{\text{lib}}$ ), we define

$$\Delta Z(S) = \sum_{i=1}^{n(S)} Z_i(S) - \sum_{i=1}^{n(R)} Z_i(R) \quad (10)$$

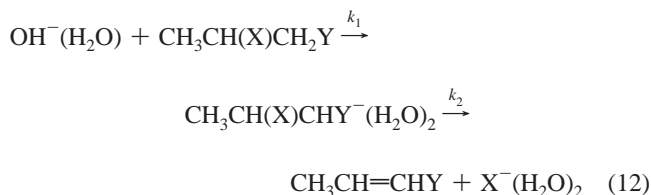
We then have

$$\Delta G(S) = \Delta G^*(S) - T\Delta S_{\text{lib}}(S) \quad (11)$$

for the value of the concentration-dependent free-energy profile at structure  $S$ . First let us consider eq 11 for standard-state concentrations and denote the standard-state concentration as  $C^\circ$ . When  $n(S) = n(R)$  and  $C_i = C^\circ$  for all  $i$ ,  $\Delta G(S)$  given by eqs 10 and 11 is independent of  $C^\circ$ . However, this is not always the case. One could nevertheless analyze the standard-state profile with values  $\Delta G_i^*(S)$  corresponding to  $C_i = 1$  mol/L for

all  $i$ . But this is artificial and does not yield the correct character of the free-energy profile for real concentrations when the number of moles changes along the reaction coordinate.

To make this clear, we refer to the reactions of interest here. The elimination reactions begin with  $\alpha$ -hydrogen abstraction by the hydroxide ion. Under the solvent conditions of interest here, ion-pairing (aggregation) should be negligible.<sup>14,15</sup> Because  $\text{OH}^-$  interacts strongly with the solvent and  $\text{B-H}$  interacts strongly with the carbanion, we rewrite the E1cB mechanism as



where  $\text{Y} = \text{CO}_2\text{CH}_3$  or  $\text{COSCH}_3$ . Thus, the free energy (pseudochemical potential) of an intermediate  $\text{I}$  is computed by treating it as a unimolecular species rather than a bimolecular one, but both the reactants ( $\text{R}$ ) and the products ( $\text{P}$ ) are treated as bimolecular. The transition state ( $\text{TS}$ ) associated with rate constant  $k_1$  is called  $\text{TS1}$ , and that associated with  $k_2$  is  $\text{TS2}$ . Thus, as one proceeds along the reaction coordinate, the structures one finds are (in order)  $\text{R}$ ,  $\text{TS1}$ ,  $\text{I}$ ,  $\text{TS2}$ , and  $\text{P}$ . We see that  $n(S) = n(\text{R})$  for  $S = \text{P}$  but not for  $S = \text{TS1}$ ,  $\text{I}$ , or  $\text{TS2}$ . We therefore set  $C_{\text{OH}^-(\text{H}_2\text{O})}$  and  $C_{\text{X}^-(\text{H}_2\text{O})_2}$  equal to typical laboratory concentrations and the other concentrations all equal to the same value, which then cancels out in  $\Delta G(S)$  at each  $S$ .

## Computational Methods and Presentation

All of the electronic structure calculations were carried out in the liquid phase with a binary ethanol/water mixture (1:1 mol/mol). The  $\text{OH}^-$  base was modeled as  $\text{OH}^-(\text{H}_2\text{O})$ , and the substrate was also explicit; these species were modeled with the M06-2X density functional,<sup>23,24</sup> the 6-31+G(d,p) basis set,<sup>30</sup> and the CM4M charge model.<sup>31</sup> For consistency, a single nonreagent water molecule was also added to all of the transition states, complexes, intermediates, and products, as in eq 12. Thus, there were two water molecules involved in the intermediates and products, one of which was derived from the reagents, in particular from the hydroxide ion and the abstracted proton. The remaining solvent molecules (water and ethanol) were implicit in a dielectric continuum surrounding the reagents and the one explicit nonreagent water molecule. The continuum solvent was modeled using the SM8 solvation model.<sup>25</sup> The electronic structure calculations were carried out using the MN-GSM module<sup>32</sup> incorporated into the *Gaussian 03* electronic structure program.<sup>33</sup> All of the stationary-point geometries were fully optimized in the reaction field<sup>20</sup> of the implicit solvent. Solution-phase vibrational frequencies were computed for each stationary point on the basis of analytical gradients and numerical Hessians. Most of the minima and transition states were confirmed to have zero and one imaginary frequency, respectively; further details are provided in the Supporting Information.

(30) Hehre, W. J.; Radom, L.; Schleyer, P. v. R.; Pople, J. A. *Ab Initio Molecular Orbital Theory*; Wiley: Hoboken, NJ, 1986.

(31) Olson, R. M.; Marenich, A. V.; Cramer, C. J.; Truhlar, D. G. *J. Chem. Theory Comput.* **2007**, *3*, 2046–2054.

(32) Olson, R. M.; Marenich, A. V.; Chamberlin, A. C.; Kelly, C. P.; Thompson, J. D.; Xidos, J. D.; Li, J.; Hawkins, G. D.; Winget, P.; Zhu, T.; Rinaldi, D.; Liotard, D. A.; Cramer, C. J.; Truhlar, D. G.; Frisch, M. J. *MN-GSM-2008*; University of Minnesota: Minneapolis, MN, 2008.

(33) Frisch, M. J.; et al. *Gaussian 03*, revision D.02; Gaussian, Inc.: Wallingford, CT, 2004.

(28) Kreevoy, M. M.; Truhlar, D. G. In *Investigations of Rates and Mechanisms of Reactions*; Bernasconi, C. F., Ed.; Techniques of Chemistry, 4th ed., Vol. 6, Part 1; Wiley: New York, 1986; pp 13–95.

(29) Truhlar, D. G. In *Isotope Effects in Chemistry and Biology*; Kohen, A., Limbach, H. H., Eds.; CRC Press: Boca Raton, FL, 2006; pp 579–619.

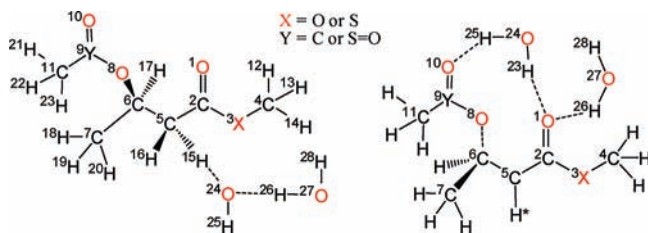


**Figure 1.** Numbering systems of anti transition states TS1 and TS2. The numbers for the hydrogen atoms attached to carbon atoms in TS2 are identical to those in TS1 except for H\*, which is  $^{15}\text{H}$  or  $^{16}\text{H}$  depending on the abstraction stereochemistry.

SM8 is a universal solvation model; that is, it is applicable to all solvents for which a few key descriptors are known. SM8 requires five solvent descriptors. For the 1:1 (mol/mol) ethanol/water solvent mixture, three of these descriptors were obtained from experimental results measured at 298 K; in particular, the dielectric constant, refractive index, and surface tension used with the solvation model were 36.7,<sup>34</sup> 1.3602,<sup>35</sup> and 36.983 cal mol<sup>-1</sup> Å<sup>-2</sup>,<sup>36</sup> respectively. The Abraham hydrogen-bond acidity and basicity parameters of water<sup>37,38</sup> were used because water molecules would be preferentially hydrogen-bonded to solutes such as hydroxide ion, esters, or thioesters.

The calculated energetics for the reactions under study are given numerically in the Supporting Information (both with and without zero-point energy) as well as in four figures in the Results; these figures show only the zero-point-inclusive values given by eq 3. The geometrical parameters at the stationary points and the partial charges on some of the atoms at the stationary points are given in the Supporting Information. All of the hydrogen-bond distances are given in Table 3. All of the tabulated free energies are relative to the value for the reactants of the reaction under consideration.

Figure 1 shows the schematic numbering system of atoms at the stationary points of the reactions. If we were to assume that all species are present at 1 M, we would have

$$\Delta G(S) = \Delta G^*(S) + 7.4 \text{ kcal/mol} \quad (13)$$

for  $S = \text{TS1}$ ,  $\text{I}$ , or  $\text{TS2}$ , whereas for  $S = \text{P}$  we would have

$$\Delta G(\text{P}) = \Delta G^*(\text{P}) - 0.5 \text{ kcal/mol} \quad (\text{substrates } \mathbf{3}\text{--}\mathbf{5}) \quad (14)$$

$$\Delta G(\text{P}) = \Delta G^*(\text{P}) - 0.6 \text{ kcal/mol} \quad (\text{substrate } \mathbf{6}) \quad (15)$$

for substrate **6**. In order to model the reaction conditions used for the experimental results that serve as the comparison for our calculations, we could assume that all species containing  $^{12}\text{C}$  and  $^{13}\text{C}$  are at the same concentration but that  $C_{\text{OH}^-(\text{H}_2\text{O})} = 1.65 \text{ M}$  and  $C_{\text{X}^-(\text{H}_2\text{O})_2} = 1.5 \text{ M}$ . Then we would have

$$\Delta G(S) = \Delta G^*(S) + 7.1 \text{ kcal/mol} \quad (16)$$

for  $S = \text{TS1}$ ,  $\text{I}$ , or  $\text{TS2}$  and

$$\Delta G(\text{P}) = \Delta G^*(\text{P}) - 0.5 \text{ kcal/mol} \quad (\text{substrate } \mathbf{3}) \quad (17)$$

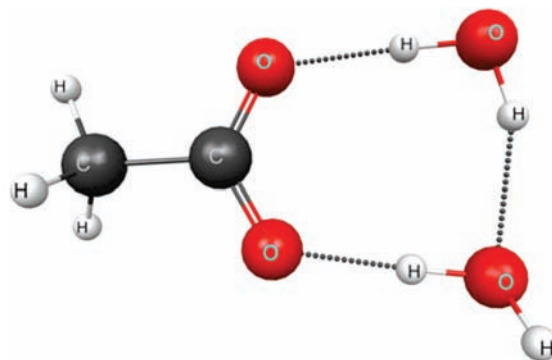


**Figure 2.** Second product (1:2 acetate/water complex) of the reactions of substrates **3** and **4**.

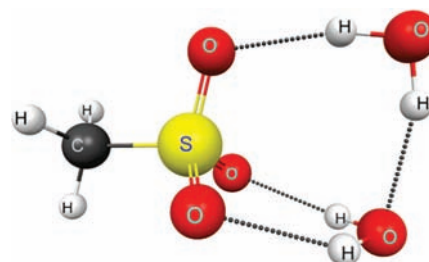


**Figure 3.** Second product (1:2 mesylate/water complex) of the reactions of substrates **5** and **6**.

$$\Delta G(\text{P}) = \Delta G^*(\text{P}) - 0.6 \text{ kcal/mol} \quad (\text{substrates } \mathbf{4}\text{--}\mathbf{6}) \quad (18)$$

One may also consider other possible reaction conditions. The reactions are usually studied under pseudo-first-order conditions. Typical conditions in ref 5 are [base] = 0.1 M and [substrate] = 5 mM.

The results in the tables and figures are  $\Delta G^*$  values (in particular, they are the  $\Delta U_0$  values, which are approximations to  $\Delta G^*$ ), which are pseudochemical potentials relative to reactants. They can be converted to values for standard or laboratory concentrations by using eqs 13–18 or eqs 6 and 10.

In order to characterize the mechanism, we have defined two subsystems. At every structure, subsystem 1 is the hydroxide, a water molecule, and the departing proton; later along the reaction path, subsystem 1 becomes two water molecules. Subsystem 2 is the remainder. If subsystems 1 and 2 were separated, subsystem 1 would have a charge of 0 and subsystem 2 a charge of  $-1$ . In our actual structures, however, the charge on subsystem 2 is not exactly  $-1$ . This is the case because for the reactants in which subsystem 2 is still bonded to the proton as well as for transition states and intermediates, the whole explicit system is a single supermolecule, and because for the products, the nucleofuge anion is complexed to two water molecules, as shown in Figures 2 and 3. The total charge on subsystem 2 was computed by adding the CM4M partial atomic charges of all the atoms of the subsystem, and it tells us how carbanion-like each structure is: a structure is very carbanion-like if the charge on subsystem 2 is close to  $-1$ . The charges on subsystem 2 are given in Table 2 to make them available for interpreting the mechanism in the following sections.

## Results

**Methyl 3-Acetoxybutanoate (3) and Methyl 3-Acetoxybutanethioate (4).** Methyl 3-acetoxybutanoate (**3**) is a good model for the deuterated acyloxy ester that was used in the earlier experimental study.<sup>14</sup> The choice of **3** as the reactant incorporated two alterations of the experimental substrate in order to simplify the calculations. The first was replacement of the *tert*-butyl ester by a methyl ester. Earlier experimental studies

(34) Sengwa, R. J.; Sankhla, M. S.; Sharma, S. *J. Solution Chem.* **2006**, *35*, 1037–1055.

(35) Herraes, J. V.; Belda, R. *J. Solution Chem.* **2006**, *35*, 1315–1328.

(36) Belda, R.; Herraes, J. V.; Diez, O. *Phys. Chem. Liq.* **2005**, *43*, 91–101.

(37) Abraham, M. H. *Chem. Soc. Rev.* **1993**, *22*, 73–83.

(38) Abraham, M. H.; Chadha, H. S.; Whiting, G. S.; Mitchell, R. C. *J. Pharm. Sci.* **1994**, *83*, 1085–1100.

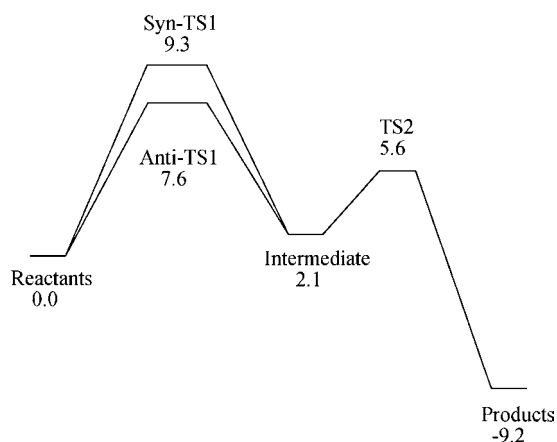
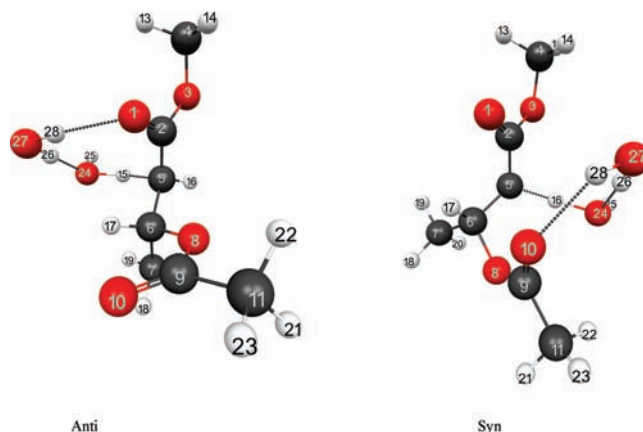
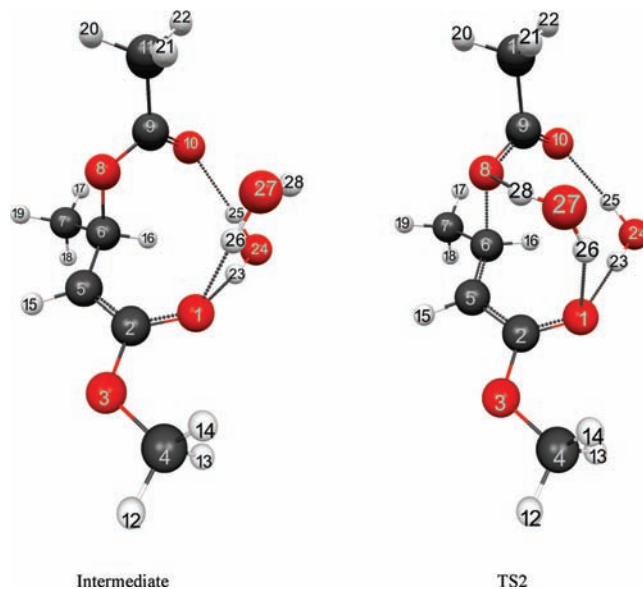
**Table 2.** CM4M Total Charges of Subsystem 2 at the Stationary Points

S	3		4		5		6	
	anti	syn	anti	syn	anti	syn	anti	syn
R	-0.11	-0.09	-0.11	-0.10	-0.11	-0.09	-0.12	-0.10
TS1	-0.45	-0.50	-0.41	-0.41	-0.44	-0.44	-0.43	-0.42
I	-0.69		-0.66		-0.79	-0.80		-0.74
TS2	-0.65		-0.64		-0.82	-0.79		-0.76
P	-0.75		-0.75		-0.85			-0.85

indicated that interchanging *tert*-butyl and ethyl groups does not change the stereochemistry of H/D exchange of  $\beta$ -substituted butanoate esters.<sup>39</sup> The second alteration was the replacement of the trimethylacetate leaving group by the acetate nucleofuge. As nucleofuges, trimethylacetate and acetate are quite comparable, but earlier experimental studies showed that under the experimental conditions, the acetoxy group could undergo both intermolecular base-initiated 1,2-elimination and a competing syn intramolecular elimination pathway, which changed the anti/syn ratio significantly.<sup>14</sup>

Figure 4 shows a schematic diagram of the energetics for the elimination pathways of **3**. This FES shows that the elimination reaction follows a two-step E1cB<sub>1</sub> pathway. The carbanion intermediate is generated by hydroxide ion abstraction of an  $\alpha$ -hydrogen, and the anti pathway is favored over the syn pathway. The free-energy barrier height for the anti TS1 is  $\sim 1.7$  kcal/mol lower than that for the syn TS1, which agrees quite well with the experimental anti/syn ratio of 20/1.<sup>14</sup> Expulsion of the acetoxy group from the enolate anion produces the product, methyl (*E*)-2-butenolate. The difference between the  $\Delta G^*$  values for the anti TS1 and TS2 is 2.0 kcal/mol. These results suggest that proton abstraction is rate-limiting, but a small amount of kinetic complexity might be present in the reaction rates (where “kinetic complexity” denotes that a single transition state is not completely rate-limiting).

The C–H bond length of the  $\alpha$ -proton is 1.10 Å in the reactant and 1.38 Å at either the anti or syn TS1, shown in Figure 5. The O–H bond distances at the anti and syn TS1s are 1.25 and 1.24 Å, respectively. A simple way to characterize the geometry of the TS is to compute the difference  $d$  between the length of the bond that is being formed at the TS and the one that is being broken. For the reactions studied here,  $d$  is  $r(\text{C–H}) - r(\text{O–H})$ . When the TS is reactant-like or product-like, the  $d$  value becomes negative or positive, respectively. The  $d$  values for the anti and syn TS1s are 0.12 and 0.14 Å,

**Figure 4.** Pseudochemical potential profile at the stationary points,  $U_0(S)$ , for **3**.**Figure 5.** Structures of the first transition states for the anti and syn elimination reactions of **3**.**Figure 6.** Intermediate and second TS for the elimination reactions of **3**.

respectively, which shows a moderately late transition state in both cases and suggests that the location of the syn TS1 may be slightly more product-like than that of the anti TS1. However, the distances between the hydroxide oxygen and the  $\alpha$ -carbon are nearly the same for the two transition states because the C–H–O angle at the syn TS1 is more linear than that at the anti TS1. The water molecule bound to the hydroxide ion in the anti TS1 forms a hydrogen bond to <sup>1</sup>O, which stabilizes the developing enolate anion. In the syn TS1, this water molecule forms a hydrogen bond to <sup>10</sup>O of the acetoxy group. The <sup>6</sup>C–<sup>8</sup>O bond of the acetoxy leaving group is changed very little as the reaction proceeds from the reactants to TS1. It is noteworthy that the <sup>6</sup>C–<sup>8</sup>O bond to the electron-withdrawing acetoxy group is nearly antiperiplanar to the <sup>5</sup>C–<sup>15</sup>H bond that is being broken.

The intermediate in the E1cB pathway of **3** is an enolate anion that is stabilized by hydrogen bonds from two water molecules, as shown in Figure 6. The hydrogen atom at <sup>5</sup>C in Figure 6 is arbitrarily denoted as <sup>15</sup>H in the intermediate and TS2; however, it would be <sup>16</sup>H from the anti TS1 and <sup>15</sup>H from the syn TS1. The CM4M partial charges show that the negative charge at <sup>1</sup>O

(39) Mohrig, J. R.; et al. *J. Am. Chem. Soc.* **1997**, *119*, 479–486.

**Table 3.** O–H Hydrogen-Bond Distances (Å) at the Stationary Points<sup>a</sup>

substrate	O–H <sup>a</sup>	anti TS1	anti SC <sup>b</sup>	syn TS1	syn SC <sup>b</sup>	O–H	int.	TS2
<b>3</b>	24–26	1.62	1.89	1.60	1.82	1–23	1.73	1.76
	1–28	1.91	1.73	2.98	2.91	1–26	1.72	1.91
	10–28	4.02	4.04	2.02	2.03	10–25	1.86	1.83
						8–28		1.93
						24–28		2.61
<b>4</b>	24–26	1.63	1.93	1.60	1.95	1–23	1.68	1.74
	1–28	2.37	1.78	2.02	1.76	1–26	1.66	1.92
	10–28	2.06	2.96	2.93	3.02	10–25	1.87	1.82
						8–28		1.95
						24–28		2.92
<b>6</b>	24–26	1.61	1.92	1.62	1.97	1–23	1.70	1.74
	1–28	1.93	1.73	2.01	1.76	1–26	1.87	1.91
						10–25	1.95	1.92
						24–28	2.14	2.11

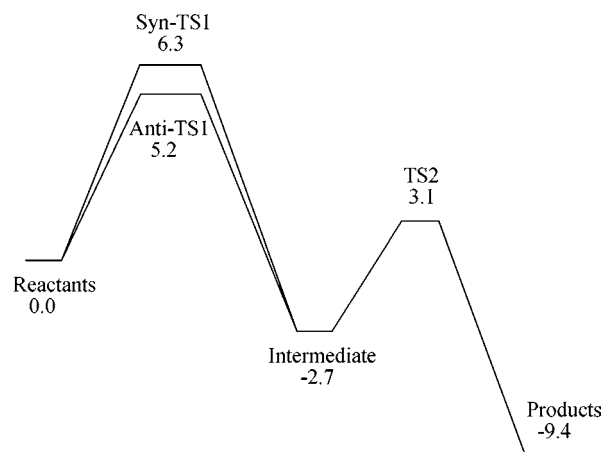
substrate	O–H	anti TS1	anti SC	syn TS1	syn SC	anti TS2	syn TS2
<b>5</b>	24–26	1.62	1.91	1.62	1.92	1.90	1.93
	1–28	1.92	1.73	2.04	1.78	1.76	1.76

<sup>a</sup> Atom numbers of the O and H atoms involved in the H bond. <sup>b</sup> SC = successor complex.

in the enolate anion is significantly greater than that in the reactant, increasing just about as much as the negative charge at the  $\alpha$ -carbon atom. Consistent with the enolate structure of the intermediate, the  $^5\text{C}-^2\text{C}$  bond distance is 0.14 Å shorter and the  $^2\text{C}-^1\text{O}$  distance 0.07 Å longer than the  $^5\text{C}-^2\text{C}$  and  $^2\text{C}-^1\text{O}$  bonds, respectively, in the reactant. In addition, the  $^6\text{C}-^5\text{C}-^2\text{C}$  bond angle increases from 112 to 120°. The total atomic charges in Table 2 show that the enolate character is larger for the intermediate than for the TS1 structures.

One expects that, all other factors being equal (for example, for the same hydrogen-bond angle), hydrogen bonds are shorter and stronger when they involve oxygens with greater negative charge. In order to make it easier to compare the hydrogen bonds in all of the structures, Table 3 provides the hydrogen-bond distances for all of the hydrogen bonds. The bond lengths for  $^1\text{O}-^{26}\text{H}$  and  $^1\text{O}-^{23}\text{H}$  in the intermediate are 1.72 and 1.73 Å, respectively, showing that these hydrogen bonds to the enolate oxygen are quite short. There is also a short hydrogen bond,  $^{24}\text{O}-^{26}\text{H}$ , at TS1. The two water molecules in the intermediate do not necessarily originate from those at TS1 because water molecules that are hydrogen-bonded to the solute can easily exchange with other water molecules from the bulk solvent; there may be numerous exchanges of water molecules in going from TS1 to the intermediate. Likewise, the two water molecules at TS2 are not necessarily those of the intermediate or of TS1. At TS2, the two hydrogen bonds to the enolate oxygen,  $^1\text{O}-^{26}\text{H}$  and  $^1\text{O}-^{23}\text{H}$ , are longer by 0.19 and 0.03 Å, respectively, whereas the  $^{10}\text{O}-^{25}\text{H}$  hydrogen bond to the acetoxy nucleofuge is shorter by 0.04 Å and an additional hydrogen bond,  $^8\text{O}-^{28}\text{H}$ , is present. Also at TS2, the  $^6\text{C}-^8\text{O}$  bond length is 1.85 Å, which is increased by 0.36 Å in comparison with that in the intermediate. The formation of the new  $^8\text{O}-^{28}\text{H}$  hydrogen bond to the acetoxy group and the shorter  $^{10}\text{O}-^{25}\text{H}$  bond assist the leaving of the nucleofuge.

Thioesters, such as methyl 3-acetoxybutanethioate (**4**), are substantially more acidic than oxygen esters. Using H–D

**Figure 7.** Pseudochemical potential profile at the stationary points,  $U_0(S)$ , for **4**.

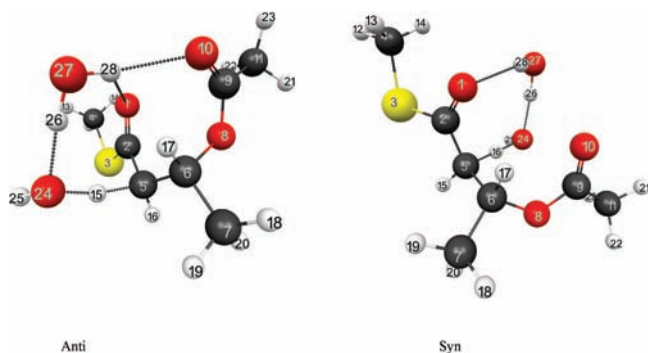
exchange kinetics, Aymes and Richard<sup>40</sup> determined the  $\text{p}K_{\text{a}}$  of ethyl thioacetate to be  $21.0 \pm 0.5$  in aqueous solution, whereas the  $\text{p}K_{\text{a}}$  of ethyl acetate was found to be  $25.6 \pm 0.5$ . Since the conjugate base of the thioester is more stable, it is expected that the  $\text{E1cB}_1$  pathway for **4** would be more favorable than the  $\text{E1cB}_1$  pathway for **3**. Figure 7 for **4** is consistent with this expectation.

Figure 7 shows the energetics for the syn and anti elimination reactions of **4** in solution. The reaction has an  $\text{E1cB}$  mechanism, but in comparison with the FES for **3** in Figure 4, the enolate intermediate is lower in energy by 4.8 kcal/mol. The change from ester to thioester reduces the barrier heights by 2.4 and 3.0 kcal/mol for the anti and syn TS1s, respectively, which is consistent with the 60-fold rate difference for the elimination reactions of *tert*-butyl 3-acetoxybutanoate and *tert*-butyl 3-acetoxybutanethioate.<sup>14</sup> The anti TS1 in **4** is 1.1 kcal/mol lower than that of the syn TS1.

In interpreting figures like Figure 7, the reader should keep in mind the earlier discussion of the concentration dependence of free energies. If we were to apply eqs 16 and 18 to Figure 7, we would see that TS1, I, and TS2 are raised 7.7 kcal/mol relative to R and P. Thus, for example, the free energy of the intermediate would be 5.0 kcal/mol higher than that of reactants under the conditions of eqs 16 and 18.

The structures of the anti and syn TS1s for the elimination reaction of **4** are presented in Figure 8. The C–H bond length for the  $\alpha$ -proton of **4** is 1.10 Å at the reactant and 1.36 and 1.33 Å at the anti and syn TS1s, respectively (as shown in Figure 8). The O–H bond distances at the anti and syn TS1s are 1.26 and 1.29 Å, respectively. Thus, the corresponding  $d$  values at the anti and syn TS1s are 0.10 and 0.04 Å, which are less positive than for **3**. The somewhat earlier transition states are not unexpected for reactions leading to a more stable intermediate. Perhaps more significantly, the location of the anti TS1 is more product-like than that of the syn TS1. This trend is also observed in the subsystem charges in Table 2; that is, for **4** the syn and anti TS1 structures have similar enolate character, whereas for **3** the syn TS is more enolate-like. The C–H–O angle at the syn TS1 for **4** is more linear than that at the anti TS1, as was also the case in the reactions of **3**. The water molecules at both transition states in **4** help to stabilize the enolate character by forming hydrogen bonds. The water

(40) Aymes, T. L.; Richard, J. P. *J. Am. Chem. Soc.* **1992**, *114*, 10297–10302; **1996**, *118*, 3129–3141.



**Figure 8.** Structures of the first transition states for the anti and syn elimination reactions of **4**.

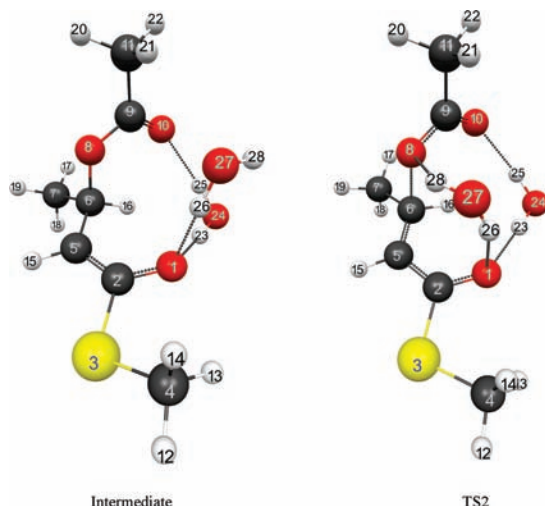


**Figure 9.** Intermediate and second TS for the elimination reactions of **4**.

molecule bound to the hydroxide ion at the anti TS1 in **4** forms two hydrogen bonds, one to  $^1\text{O}$  and the other to  $^{10}\text{O}$ , but that at the syn TS1 makes only one hydrogen bond, to  $^1\text{O}$ . Table 3 shows that the  $^1\text{O}-^{23}\text{H}$  hydrogen bond at the syn TS1 is shorter than that at the anti TS1. As in the case of the methyl 3-acetoxybutanoate reaction, the  $^6\text{C}-^8\text{O}$  bond length to the acetoxy nucleofuge remains nearly the same as the reaction goes from reactant to intermediate, increasing by only 0.03 Å, which also is consistent with the stepwise E1cB mechanism for **4**. The  $^6\text{C}-^8\text{O}$  bond to the electron-withdrawing acetoxy group is farther from an antiperiplanar arrangement to the  $^5\text{C}-^{15}\text{H}$  bond being broken in the anti TS1 of **4** than was the case with **3** (148 vs 167°, respectively). Although the extent of deviation from antiperiplanarity is larger than expected, the motions are soft.

The enolate anion intermediate in the E1cB pathway of **4**, shown in Figure 9, is stabilized by two short hydrogen bonds. The  $^1\text{O}-^{23}\text{H}$  and  $^1\text{O}-^{26}\text{H}$  hydrogen-bond lengths in Figure 9 are 1.68 and 1.66 Å, respectively. Consistent with the enolate structure, the  $^5\text{C}-^2\text{C}$  bond distance is 0.16 Å shorter and the  $^2\text{C}-^1\text{O}$  distance 0.08 Å longer than the corresponding  $^5\text{C}-^2\text{C}$  and  $^2\text{C}-^1\text{O}$  bonds in the reactant. In addition, the  $^6\text{C}-^5\text{C}-^2\text{C}$  bond angle has increased from 111 to 120°. One would expect there to be a high barrier to rotation about the enolate anion  $^5\text{C}-^2\text{C}$  bond. As shown in Figure 9, the  $^6\text{C}-^8\text{O}$  bond in the enolate intermediate for the reaction of **4** (like that in the case of **3**) is orthogonal to the planar  $^5\text{C}-^2\text{C}-^1\text{O}$  substructure of the

enolate anion, which would allow for stabilization by negative hyperconjugation.<sup>41,42</sup>

TS2 for the elimination reaction of **4** has geometric parameters similar to those at TS2 for **3**, except that the  $^6\text{C}-^8\text{O}$  bond length is 0.05 Å longer for **4**. In the reaction of **4**, the energy barrier in going from the intermediate to TS2 is substantially larger, mainly as a result of the greater stability of the thioester conjugate base. This barrier of 5.8 kcal/mol would give the enolate intermediate a substantially longer lifetime. Nonetheless, as long as there is no return to the reactants and the driving force to produce the *trans*-alkene is strong, rotation about the  $^5\text{C}-^6\text{C}$   $\sigma$  bond in the intermediate enolate anion should not affect the stereochemical outcome of the elimination reaction.

The  $^6\text{C}-^8\text{O}$  bond length to the acetoxy nucleofuge is 1.90 Å at TS2, which is larger than the  $^6\text{C}-^8\text{O}$  bond in the intermediate by 0.42 Å. At the same time, the hydrogen bonds  $^1\text{O}-^{26}\text{H}$  and  $^1\text{O}-^{23}\text{H}$  are longer than those in the intermediate by 0.25 and 0.06 Å, respectively, whereas the  $^{10}\text{O}-^{25}\text{H}$  hydrogen bond to the acetoxy nucleofuge is shorter by 0.06 Å and an additional hydrogen bond,  $^8\text{O}-^{28}\text{H}$ , is present. This new hydrogen bond and the shorter  $^{10}\text{O}-^{25}\text{H}$  bond assist the leaving of the acetate nucleofuge.

**Methyl 3-Mesyloxybutanoate (5) and Methyl 3-Mesyloxybutanethioate (6).** In order to further assess the usefulness of our computational study for providing mechanistic insights, we did calculations on the hydroxide ion-catalyzed 1,2-elimination reactions of a  $\beta$ -methanesulfonyloxybutanoate ester (**5**) and the analogous thioester (**6**). The sulfonate nucleofuges are excellent leaving groups, among the best for which rates of elimination reactions have been studied.<sup>43</sup> The experimental study we modeled with **5** and **6** used stereospecifically deuterated ( $2R^*,3R^*$ )-**2a** and its ( $2R^*,3S^*$ ) diastereomer, as well as the analogous thioesters **2b**, where the pathway was proposed as E2 with an E1cB-like transition state.<sup>15</sup> In order to simplify the calculations, mesyloxy ( $\text{MeSO}_2\text{O}$ )-substituted reactants were used rather than the tosyloxy ( $\text{CH}_3\text{C}_6\text{H}_4\text{SO}_2\text{O}$ )-substituted reactants from the experiments. A comparison of the effects of mesylate and tosylate leaving groups on the rates of ethoxide-catalyzed elimination reactions of  $\beta$ -substituted phenyl sulfones, which are thought to follow an E1cB<sub>1</sub> pathway, showed that the mesyloxy substrates reacted slightly faster, by a factor of 1.7.<sup>44</sup> As nucleofuges, methanesulfonate and toluenesulfonate are quite comparable.

Figure 10 shows a schematic diagram of the energetics for the elimination pathways of **5** to methyl (*E*)-2-butenolate and methanesulfonate anion (Figure 3). The FES is most consistent with an E2 pathway having an E1cB-like transition state, similar to that proposed for the tosyloxy reactant. The free-energy barrier height for the anti TS1 is  $\sim 1.2$  kcal/mol lower than that for the syn TS1, which agrees reasonably well with the experimental anti/syn ratio of 17/1.<sup>15</sup> The absolute barrier heights for TS1, however, are slightly greater than the analogous barrier heights calculated for **3** (shown in Figure 4). This does not compare well with the experimental second-order rate constants for the elimination reactions of the  $\beta$ -OTs and  $\beta$ -OAc reactants, where  $k_2$  for the  $\beta$ -OTs compound is 63 times the rate constant for the  $\beta$ -OAc compound.

(41) Thibblin, A. *Chem. Scr.* **1980**, 121–127.

(42) Meng, Q.; Thibblin, A. *J. Chem. Soc., Perkin Trans. 2* **1998**, 583–589.

(43) Stirling, C. J. M. *Acc. Chem. Res.* **1979**, 12, 198–203.

(44) Marshall, D. R.; Thomas, P. J.; Stirling, C. J. M. *J. Chem. Soc., Perkin Trans. 2* **1977**, 1914–1919.



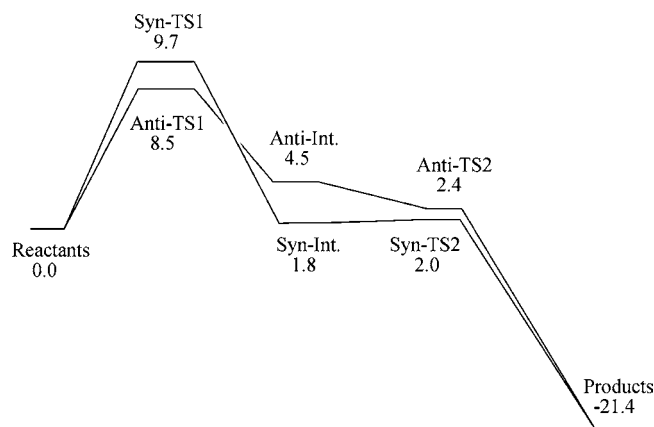


**Figure 10.** Pseudochemical potential profile at the stationary points,  $U_0(S)$ , for **5**. In schematic diagrams like this one, the structures labeled as intermediates can be either putative or actual intermediates, and the lines connecting structures are just to guide the eye; for example, the actual reaction path from the anti TS2 goes to a lower-energy structure than the one labeled “Anti-Int.,” which is a successor complex from the syn TS1.

The structures of the anti and syn TS1s for the elimination reaction of **5** are presented in Figure 11. The C–H bond length of the  $\alpha$ -proton was calculated to be 1.10 Å at the reactant and 1.35 and 1.34 Å at the anti and syn TS1, respectively. The O–H bond distances at the anti and syn TS1s were calculated to be 1.28 and 1.29 Å, respectively. The corresponding  $d$  values for the anti and syn transition states are 0.07 and 0.05 Å, which are somewhat less positive than those for **3** and **4**, with the anti TS1 somewhat more product-like. Table 3 shows that the  $^1\text{O}-^{28}\text{H}$  hydrogen bond at the anti TS1 is shorter than that at the syn TS1, again suggesting that the anti TS1 is more enolate-like. The C– $^{16}\text{H}$ –O angle at the syn TS1 is more linear than the C– $^{15}\text{H}$ –O angle at the anti TS1, which is consistent with the previous two reactions. Only one hydrogen bond is formed between the  $^1\text{O}$  atom and the water molecule bound to the hydroxide ion at both TS1 structures, which helps to stabilize the enolate-like character at TS1. The longer  $^1\text{O}-^{28}\text{H}$  hydrogen-bond distance and larger negative partial charge on the  $^1\text{O}$  atom at the syn TS1 relative to those at the anti TS1 are correlated with the O–H– $^1\text{O}$  hydrogen-bond angles. A larger angle (closer to linear) correlates with a stronger hydrogen bond; the O–H– $^1\text{O}$  angles at the anti and syn TS1s are 160 and 151°, respectively (the former is listed in Table S6 in the Supporting Information), and as a result, the hydrogen bond in the syn TS1 is longer and weaker. All attempts to locate the most stable intermediate structure with two hydrogen bonds on the  $^1\text{O}$  atom resulted in breaking of the  $^6\text{C}-^8\text{O}$  bond and formation of the alkene product.

The  $^6\text{C}-^8\text{O}$  bond of the mesyloxy leaving group is lengthened by only 0.01 Å at TS1 relative to that in the reactant. Thus, the transition states for the E2 elimination from the mesyloxy ester **5** are highly asynchronous and very E1cB-like. The  $^6\text{C}-^8\text{O}$  bond to the electron-withdrawing mesyloxy group is 17° away from being antiperiplanar to the  $^5\text{C}-^{15}\text{H}$  bond being broken in the anti TS1 (see the above comment regarding the softness of motion in this degree of freedom) and is synperiplanar to the  $^5\text{C}-^{16}\text{H}$  bond being broken in the syn TS1.

Figure 12 summarizes the energetics and stationary points for methyl 3-mesyloxybutanethioate (**6**). Since the conjugate base of the thioester is more stable than the enolate of ester **5**, it is expected that the E1cB<sub>1</sub> pathway for **6** would be more favorable than the E1cB<sub>2</sub> pathway for **5**. Figure 12 is consistent

with this expectation. Also consistent with the excellent sulfonate nucleofuge, Figure 12 shows that the putative intermediate enolate anion from mesyloxy thioester **6** has a lower free-energy barrier to reach TS2 (1.6 kcal/mol) than is the case with the acetoxy thioester **4** (5.8 kcal/mol), and this barrier is so small that it is doubtful whether this structure is a kinetically significant intermediate. At 1.55 Å, the  $^6\text{C}-^8\text{O}$  bond of the intermediate enolate anion is longer by 0.06 Å than the  $^6\text{C}-^8\text{O}$  bond in the anti TS1. A  $^{10}\text{O}-^{25}\text{H}$  hydrogen bond assists the leaving of the nucleofuge. It is probable that the barrier of the second step in this reaction is so small that the rate may be comparable to the rate of water exchange in the bulk solvent (i.e., the rate of hydrogen-bond formation with other water molecules).

The structures of the anti and syn TS1s for the elimination of **6** are shown in Figure 13. The C–H bond length of the  $\alpha$ -proton is 1.33 Å at both the anti and syn TS1s, and the O–H bond distance at both TS1 structures is 1.30 Å. The location of the anti TS1 is slightly more product-like than that of the syn TS1. Consistent with the previous reactions, the C–H–O angle of the syn TS1 is more linear than that of the anti TS1. In both the anti and syn TS1s, there is only one hydrogen bond to the  $^1\text{O}$  atom from the water molecule bound to hydroxide. Table 3 shows that the  $^1\text{O}-^{28}\text{H}$  hydrogen bond at the anti TS1 is slightly shorter than that at the syn TS1. The  $^6\text{C}-^8\text{O}$  bond length of the mesyloxy leaving group increases continuously in going from reactant to TS1 to intermediate (shown in Figure 14), but the variation is not large, which again suggests the stepwise E1cB mechanism. As was the case for the reactions of both **3** and **4**, Figure 14 shows that the  $^6\text{C}-^8\text{O}$  bond in the enolate intermediate in the reaction of **6** is nearly antiperiplanar to the planar  $^5\text{C}-^2\text{C}-^1\text{O}$  substructure of the enolate anion.

The  $^6\text{C}-^8\text{O}$  bond length at TS2 is 1.71 Å, which is short in comparison with that in the previous reactions involving the acetate nucleofuge and points to an early transition state, consistent with the large exergonicity in the second step. It is interesting to note that cyclic hydrogen bonds are formed by two water molecules in the intermediate and at TS2, as shown in Figure 14. The  $^1\text{O}-^{23}\text{H}$  hydrogen bond length in the intermediate is 1.70 Å, indicating a large partial negative charge on the  $^1\text{O}$  atom of the enolate anion, which is also consistent with the CM4M partial charges.

The barrier height for the anti TS1 from **6** is only 0.1 kcal/mol lower than that for the syn TS1; thus, there is almost no difference in the barrier heights for anti and syn elimination in this reaction. This contrasts with the experimental result of a 16/1 anti/syn ratio observed using stereospecifically labeled **2b**.<sup>15</sup> The substitution of ester **5** by thioester **6** also reduces the barrier heights by 2.6 and 3.7 kcal/mol for the anti and syn TS1s, respectively, which reflects to some extent the 18-fold difference in the rate constants for **5** and **6**. We found that  $\Delta G^*$  for TS2 is –1.1 kcal/mol, which is 7.0 kcal/mol lower than that for the anti TS1. These results, especially when considered in conjunction with the size of the free-energy barrier from the putative intermediate to TS2, suggest that the first step is rate-limiting for both the anti and syn eliminations without kinetic complexity.

In the reactions of **3–6**, the  $^5\text{C}-^6\text{C}$  bond length decreases from 1.52 Å in the reactants to 1.49–1.51 Å at all eight first transition states but shows greater variation at the second

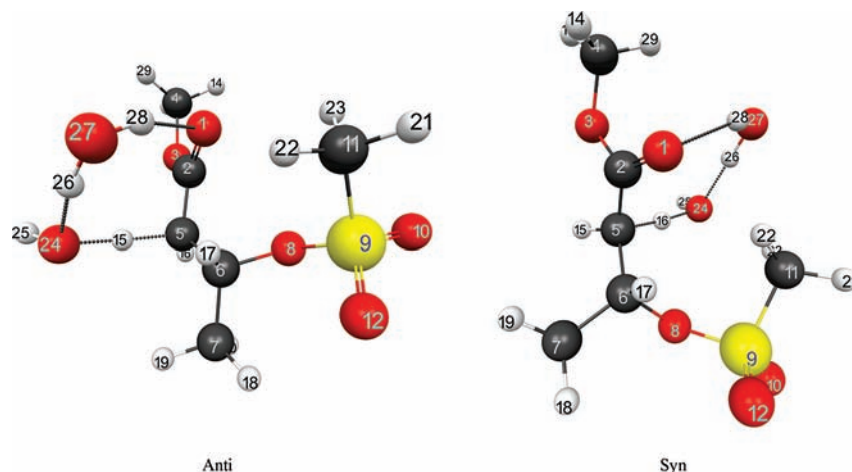


**Figure 11.** Transition-state structures for the anti and syn elimination reactions of **5**.

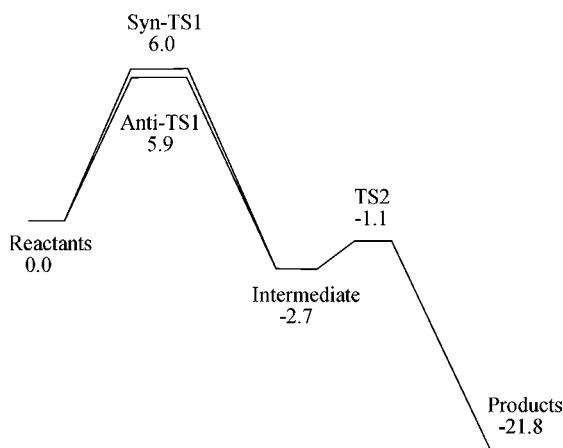


**Figure 12.** Pseudochemical potential profile at the stationary points,  $U_0(S)$ , for **6**

transition states, for which it decreases to 1.40 Å for carboxylate leaving groups and 1.42–1.44 Å for sulfonate leaving groups.

## Discussion

Understanding the factors underlying the diversity of mechanisms for chemical transformations in the condensed phase is a key step in achieving an understanding of reactivity and substituent effects and designing new reactions and catalysts. Many traditional explanations have focused on the qualitative effect of a factor such as the energy of reaction, steric hindrance, hydrogen bonding, or electrostatic solvation, but the quantitative effects of any of these factors on rate constants and relative rate constants are entirely contained in their effect on the free energies of activation and the transmission coefficients of the reaction under consideration. In most cases, except when tunneling effects are important, if the transition state is identified variationally on the FES rather than on the gas-phase internal energy surface, the transmission coefficients are expected to be close to unity, and the determining factor becomes the free energy of activation.

Electronic effects and solvent interactions play critical roles in determining the mechanisms of ionic reactions.<sup>45</sup> The emergence of chemically accurate density functionals<sup>23,24,46</sup> and quantitative solvation models<sup>25,47</sup> means that we can explore free energies of activation for competing mechanisms in solution-phase reactions more reliably than previously by using

full calculations of the stationary points of the FES in liquid-phase solutions. The present article has presented a systematic approach for this kind of calculation and illustrated it by calculations on one of the classic problems of physical organic chemistry, namely, the competition between concerted and nonconcerted elimination reactions. Many computational studies on the mechanisms of base-catalyzed 1,2-elimination reactions have been carried out, but until recently, it was not possible to include quantitatively realistic specific solvent effects. In the present study, we have focused on internal energy and solvation free energy and not considered tunneling and variational effects. In particular, we have combined a kinetically well-validated density functional treatment of the solute and two explicit solvent molecules with a universal implicit solvation model for a polar solvent mixture.

Attempts to resolve the issue of assigning E2 and E1cB pathways for elimination reactions have been controversial for over 50 years. The actual mechanisms form a spectrum of pathways that extends from fully synchronous, as well as concerted, E2 to a fully formed enolate intermediate with a significant energy minimum. In between, there is a range of mechanisms that, as the substrate is varied, may look more and more E1cB-like. At the borderline, the transition states of the two kinds of mechanism may smoothly merge;<sup>48</sup> an alternative scenario is that there is a sharp transformation of the mechanism.<sup>49</sup>

In 1972, Bordwell concluded that most base-initiated  $\beta$ -eliminations involving activation by an electron-withdrawing group, such as a carbonyl group, proceed by E1cB mechanisms rather than by concerted E2 mechanisms.<sup>1</sup> A good deal of subsequent experimental work has borne out this conclusion. Our computational studies are in agreement with Bordwell's conclusion for the reactions of ester **3** and thioesters **4** and **6**.

(45) For example, see: (a) Ohisa, M.; Yamataka, H.; Dupuis, M.; Aida, M. *Phys. Chem. Chem. Phys.* **2008**, *10*, 844. (b) Kim, Y.; Cramer, C. J.; Truhlar, D. G. *J. Phys. Chem. A* **2009**, *113*, 9109. (c) Chen, X.; Regan, C. K.; Craig, S. L.; Krenske, E. H.; Houk, K. N.; Jorgensen, W. L.; Brauman, J. I. *J. Am. Chem. Soc.* **2009**, *131*, 16162.

(46) (a) Zhao, Y.; González-García, N.; Truhlar, D. G. *J. Phys. Chem. A* **2005**, *109*, 2012. (b) Zheng, J.; Zhao, Y.; Truhlar, D. G. *J. Chem. Theory Comput.* **2009**, *5*, 808.

(47) Cramer, C. J.; Truhlar, D. G. *Acc. Chem. Rev.* **2008**, *41*, 760.

(48) Mosconi, E.; De Angelis, F.; Belpassi, L.; Tarantelli, F.; Alunni, S. *Eur. J. Org. Chem.* **2009**, 5501–5504.

(49) (a) Jia, Z. S.; Rudzinski, J.; Paneth, P.; Thibblin, A. *J. Org. Chem.* **2002**, *67*, 177–181. (b) Cho, B. R.; Jeong, H. C.; Seung, Y. J.; Pyun, S. Y. *J. Org. Chem.* **2002**, *67*, 5501–5504.

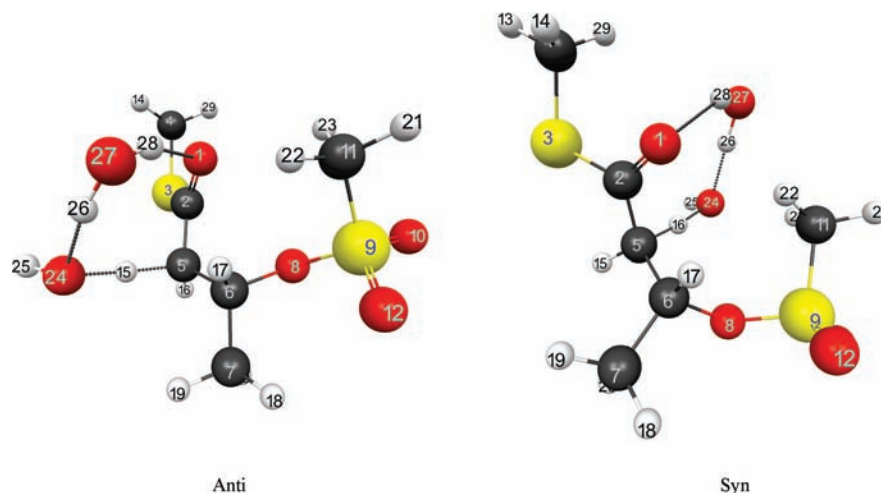


Figure 13. Structures of the first transition states for the anti and syn elimination reactions of **6**.

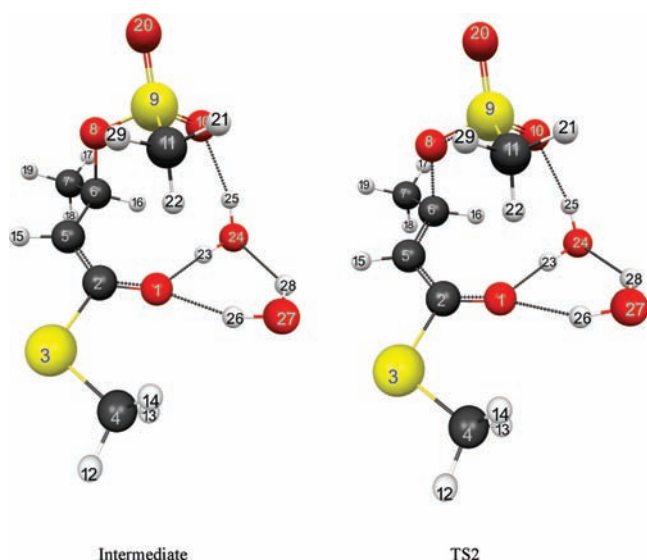


Figure 14. Intermediate and second TS for the elimination reactions of **6**.

The bond angles and bond lengths in these E1cB<sub>1</sub> pathways are consistent with enolate anion intermediates. The most stable conformations of the enolate anions have the <sup>6</sup>C–<sup>8</sup>O bond to the leaving group nearly orthogonal to the <sup>5</sup>C–<sup>2</sup>C–<sup>1</sup>O substructure, which would allow for stabilization by negative hyperconjugation.

In the case of the mesyloxyester **5**, the calculations as well as earlier experimental evidence<sup>15</sup> favor a concerted but asynchronous E2 mechanism with an E1cB-like transition state. The elimination of methanesulfonic acid from **5** involves base abstraction of a proton α to the carbonyl group of an ester, which is less acidic than an α-proton of a thioester, and the expulsion of a β-methanesulfonyloxy group, an excellent nucleofuge. Thus, we might expect the base-catalyzed 1,2-elimination pathway of **5** to be as likely a candidate as any β-elimination involving activation from a carbonyl group for a possible asynchronous E2 mechanism with an E1cB-like transition state.

Some years ago, Jencks pointed out that the transformation of an E1cB pathway into an E2 pathway occurs when the carbanion intermediate disappears because it becomes too unstable to exist. When that happens, a stepwise mechanism is

impossible, and a concerted mechanism is enforced.<sup>50</sup> Three different situations need to be considered in this change of mechanism. The possibility that the E1cB and E2 pathways coexist and that the mechanism proceeds through a mixture of pathways seems unlikely in the general case.<sup>50b,51</sup> A question then arises as to whether the change from a stepwise to a concerted mechanism is sharp or smooth. Whereas the kinetic analysis of Gandler and Jencks<sup>51</sup> supported a sharp transformation, with the two reaction pathways occurring on unrelated regions of the energy surface, the recent kinetic data and computational studies of Alunni and co-workers strongly support a smooth continuum between the E1cB and E2 pathways.<sup>48,52</sup>

With a continuum from central E2 pathways to E1cB pathways having fully formed carbanion intermediates at significant energy minima, what is the point in the continuum that distinguishes a concerted but asynchronous E2 pathway with an E1cB-like transition state from an E1cB pathway with a kinetically significant carbanion intermediate? In other words, for the purposes of classifying a reaction mechanism, when is a putative intermediate not an actual intermediate? Our inability to locate a hydrogen-bond-stabilized enolate intermediate on the FES for the elimination pathway for **5**, which does not result in breaking of the C–O bond to the mesyloxy nucleofuge and formation of the alkene product, is consistent with our interpretation that **5** reacts by an asynchronous E2 mechanism with an E1cB-like transition state. Nevertheless, there is an inherent ambiguity in this conclusion: when the transition is gradual, there is no precise border. It is possible that a short-lived carbanion exists even though there is no local minimum in the FES. The treatment here would not attribute any kinetic significance to such an intermediate in conventional rate constant measurements, although in principle it could be observed in single-molecule studies.<sup>53</sup>

There is, however, the possibility that our reaction coordinate is too simplified. For example, we did not consider the possibility of a short-lived carbanion whose lifetime is deter-

(50) (a) Jencks, W. P. *Chem. Soc. Rev.* **1981**, *10*, 345–375. (b) Banait, N. S.; Jencks, W. P. *J. Am. Chem. Soc.* **1990**, *112*, 6950–6958.

(51) Gandler, J. R.; Jencks, W. P. *J. Am. Chem. Soc.* **1982**, *104*, 1937–1951.

(52) (a) Alunni, S.; De Angelis, F.; Ottavi, L.; Papavasileiou, M.; Tarantelli, F. *J. Am. Chem. Soc.* **2005**, *127*, 15151–15160. (b) De Angelis, F.; Tarantelli, F.; Alunni, S. *J. Phys. Chem. B* **2006**, *110*, 11014–11019.

(53) Luchian, T.; Shin, S.-H.; Bayley, H. *Angew. Chem., Int. Ed.* **2003**, *42*, 1926–1929.

mined by a collective solvent relaxation. Near the saddle point of the FES, our reaction coordinate is the imaginary-frequency normal mode of the supersolute, and it therefore includes at most two water molecules. If additional water molecules participate in the reaction coordinate, then in principle there could be a second maximum in the free energy of activation profile that is associated with solvent relaxation coupled to the dissociation of the conjugate base, which would convert the conjugate base from a fleetingly populated configuration along the reaction path to an intermediate. Such an effect is an example of nonequilibrium solvation, as discussed elsewhere.<sup>54</sup>

A concerted asynchronous E2 pathway for the base-catalyzed 1,2-elimination of mesyloxyester **5** is also more consistent with the *E/Z* ratio of the alkene products with sulfonyloxy leaving groups in comparison with that in eliminations using poorer leaving groups.<sup>15</sup> Base-catalyzed elimination of *p*-toluene-sulfonic acid from simple secondary alkyl tosylates under non-ion-pairing conditions normally produces 15–35% (*Z*)-alkene by the E2 pathway, with the range reflecting steric effects as well as the relative stability of the *E* and *Z* isomers.<sup>15</sup> In comparison with those of simple acyclic alkenes, the *E* isomers of *tert*-butyl 2-butenate and its thioester are substantially more stable than the *Z* isomers, and the elimination reactions of stereospecifically deuterated butanoate esters and thioesters with  $\beta$ -carboxyl leaving groups produce  $\sim$ 1.5% (*Z*)-alkene.<sup>14</sup> Use of the poorer *m*-trifluoromethylphenoxy nucleofuge produces 0.5–1.3% (*Z*)-alkene. The elimination studies on substrates with these poorer leaving groups indicate that they follow an irreversible stepwise E1cB pathway. However, there is a 4–5-fold increase in the percentage of (*Z*)-alkene when the tosyloxy group is the nucleofuge, which is consistent with the proposal that the elimination reactions with sulfonyloxy leaving groups are near the E2 borderline.<sup>15</sup> It remains unclear what factors lead to more (*Z*)-alkene product in an E2 pathway.

A better nucleofuge and greater acidity of the  $\alpha$ -proton speed up the reaction, but the effects on the *syn/anti* ratio are less systematic. The *anti* elimination pathway was calculated to be preferred for all of the reactants we studied, which agrees well with experiment.<sup>14,15</sup> Contrary to earlier suggestions, the present calculations predict that the *anti* pathway is preferred over the *syn* pathway even for the more acidic thioesters.

Strong *anti/syn* discrimination is present in the reactions of substrates **3**, **4**, and **6** even though they proceed through enolate intermediates with significant free-energy barriers for expulsion of the nucleofuge. Because the reprotonation of the enolate anion is slow and the driving force to the (*E*)-alkene is much greater than that for formation of the (*Z*)-alkene, the stereochemical determinant for *anti/syn* discrimination is which of the two  $\alpha$ -protons is abstracted by the base. Under these constraints, abstraction of the proton determines the configuration at  $^5\text{C}$  of

the enolate anion, and rotation about the  $^5\text{C}-^6\text{C}$   $\sigma$  bond does not change the stereochemical result in the formation of the predominant (*E*)-alkene product.

## Concluding Remarks

After presenting a general formalism for using free-energy surfaces to model liquid-phase reactions, including both explicit and implicit solvation, we have illustrated the formalism by studying structurally related, base-initiated elimination reactions that produce conjugated esters and thioesters using two nucleofuges with different leaving-group abilities. For all four substrates, the calculations correlate with experimental rate differences for both stereoselectivity and rate and provide useful mechanistic insights. For example, earlier theoretical treatments of elimination stereoselectivity suggested that *syn* elimination is expected to become more competitive for transition states with extensive carbanion character, but our calculations confirm the experiments that refute this.

Our computational study found similar mechanisms and free-energy profiles for the four substrates, but there are also important differences. We found an irreversible stepwise E1cB<sub>1</sub> mechanism for acetoxy ester **3** and thioester **4** as well as for mesyloxy thioester **6**. However, no intermediate could be found for mesyloxy ester **5**, which seems to follow a concerted but asynchronous E2 mechanism with an E1cB-like transition state. This is consistent with the finding<sup>15</sup> that the ratios of (*Z*)- to (*E*)-alkene products for the tosyloxy ester and thioester are much larger than those for the carboxylate and *m*-trifluoromethylphenoxy leaving groups, which have kinetically important enolate intermediates.

Furthermore, the calculations have provided structural and electrostatic information that is not available experimentally, although many experiments whose sole objective was to gain indirect information from which such geometrical structures and charge distributions could be inferred have been reported. We found that a hydrogen-bond network involving two water molecules stabilizes all of the transition states and intermediates by diffusing the negative charge and also that hydrogen bonding assists in expulsion of the nucleofuge.

**Acknowledgment.** This work was supported in part by the National Science Foundation through Grant CHE09-56776.

**Supporting Information Available:** Relative free energies for elimination reactions computed using SM8/CM4M/M06-2X/6-31+G(d,p); geometric parameters and CM4M partial charges at stationary points; pseudochemical potential profiles  $U_0(S)$  at all stationary points, including successor complexes, for **3**–**6**; absolute energies of calculated structures; and complete refs 33 and 39. This material is available free of charge via the Internet at <http://pubs.acs.org>.

JA101104Q

(54) Truhlar, D. G. In *Isotope Effects in Chemistry and Biology*; Kohen, A., Limbach, H.-H., Eds.; CRC Press: Boca Raton, FL, 2006; p 593.